

# Constructing new seismograms from old earthquakes: Retrospective seismology at multiple length scales

Elizabeth Entwistle<sup>1</sup>, Andrew Curtis<sup>1</sup>, Erica Galetti<sup>1</sup>, Brian Baptie<sup>2</sup> & Giovanni Meles<sup>1</sup>

1. School of GeoSciences, University of Edinburgh, Grant Institute, James Hutton Road, The King's Buildings, Edinburgh, EH9 3FE

2. British Geological Survey, Murchison House, West Mains Road, Edinburgh, EH9 3LA



Contact:

elizabethentwistle09@gmail.com

## 1. Introduction

If energy emitted by an earthquake is recorded on a suitable backbone array of seismometers, source-receiver interferometry (SRI) is a method that allows those recordings to be projected to the location of another target seismometer, providing an estimate of the seismogram that would have been recorded at that location. Since the other seismometer may not have been deployed at the time the source occurred, this renders possible the concept of “retrospective seismology” whereby the installation of a sensor at one period of time allows the construction of virtual seismograms as though that sensor had been active before or after its period of installation. Using the benefit of hindsight of earthquake location or magnitude estimates, SRI can establish new measurement capabilities closer to earthquake epicenters, potentially improving earthquake location estimates (Entwistle et al., 2015).

## 2. Source-Receiver Interferometry (SRI)

Correlation-correlation SRI, as shown in Figure 1a can be described by the coupling of noise interferometry and inter-source interferometry in Equations 1 and 2 (Curtis et al., 2012; Entwistle et al., 2015). This coupling allows earthquake energy recorded on array seismometers  $x$  from a source at  $s$  on fault plane  $F$ , with source time signature  $T(\omega)$ , to be both spatially and temporally redatumed to a target sensor at  $r$ :

$$1) G_H(x, r) \cong Cv^*(r)v(x)$$

$$2) \int_{s \in F} T(s)^* G_H(r, s) ds \cong \frac{2jk}{\omega\rho} \int_S \int_{s \in F} [T(s)G(x, s)]^* G(x, r) ds dx$$

Where  $C$  is a constant and  $v$  is the ambient noise field fluctuations recorded on  $x$  and  $r$  from locations such as  $x'$  on boundary  $S'$  (Wapenaar and Fokkema, 2006). Equation 2 describes waves of angular frequency  $\omega$  and wavenumber  $k$  propagating in an acoustic medium with density  $\rho$ .  $j = \sqrt{-1}$  and  $G_H$  is the homogeneous Green's function.

For correlation-convolution SRI, as shown in Figure 1b, correlation on the right of Equation 2 is replaced by convolution such that:

$$3) \int_{s \in F} T(s)G(r, s) ds \cong \frac{2jk}{\omega\rho} \int_S \int_{s \in F} T(s)G(x, s)G(x, r) ds dx$$

Only those array seismometers that provide a stationary phase contribution to the integrals in Equations 2 and 3 are required at locations  $x$  (Snieder, 2004). The regions of boundary  $S$  that they occupy are highlighted in Figure 1 by the thick grey lines.

To best approximate the integration over the receiver boundary  $S$  in Equations 2 and 3 we:

1. Embed array seismometers  $x$  within Voronoi cells (Figure 2b)
2. Apply 2D cosine tapers to the tessellation boundary
  - Invokes the stationary phase approximation (Snieder 2004)
  - Reduces boundary effects

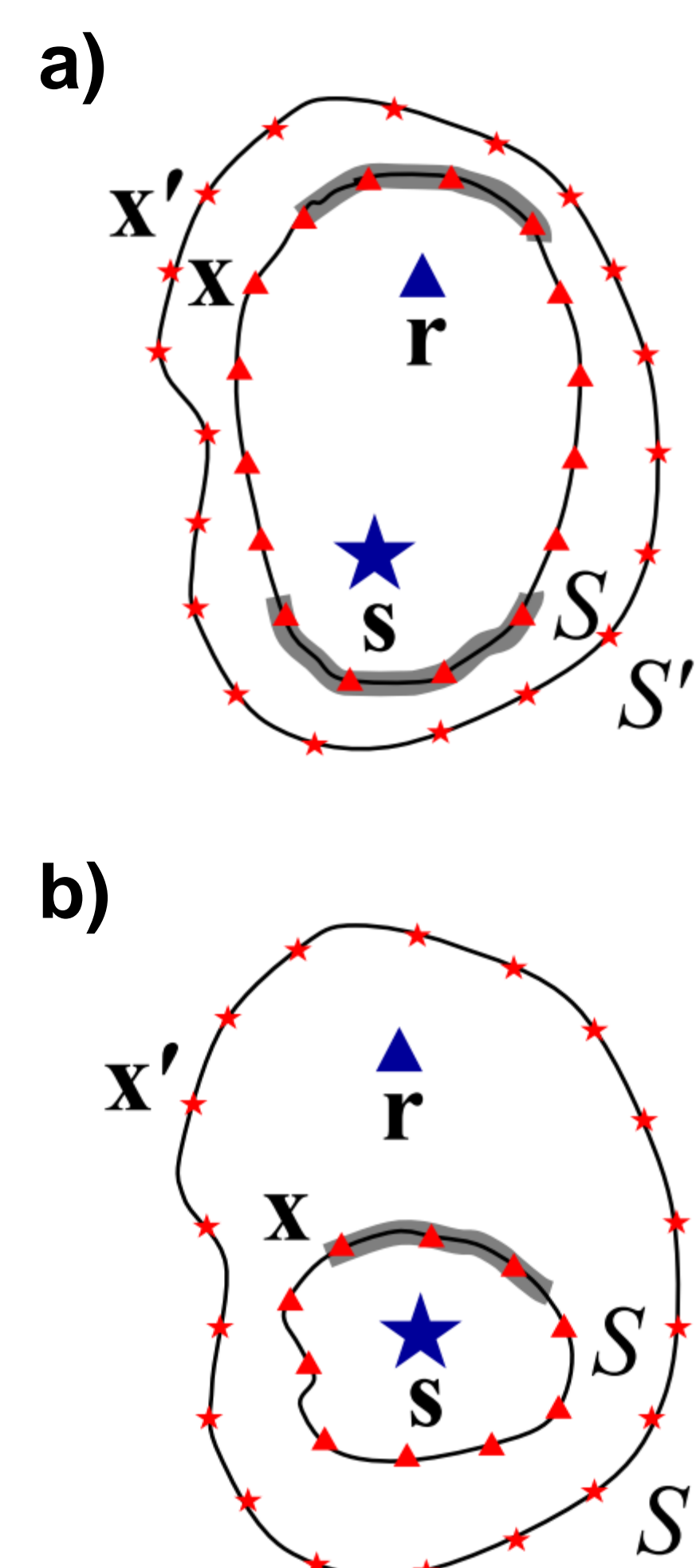


Figure 1: Schematic geometries pertaining to: a) correlation-correlation SRI, and b) correlation-convolution SRI. See symbol key below

- ▲ Target sensor
- ★ Earthquake source
- ★ Ambient noise sources
- ▲ Array seismometers
- Necessary array seismometers

## 3. Results

Virtual seismograms of a M 6.5 earthquake that occurred off the coast of California are constructed on target sensors **WDC**, **BMN**, **DUG**, **P21A**, **R29A**, **R30A**, **R31A** and **GOGA** (Figures 2c-e) using array seismometers embedded within Voronoi cells (Figure 2b), and Equations 1 and 2 or 3.

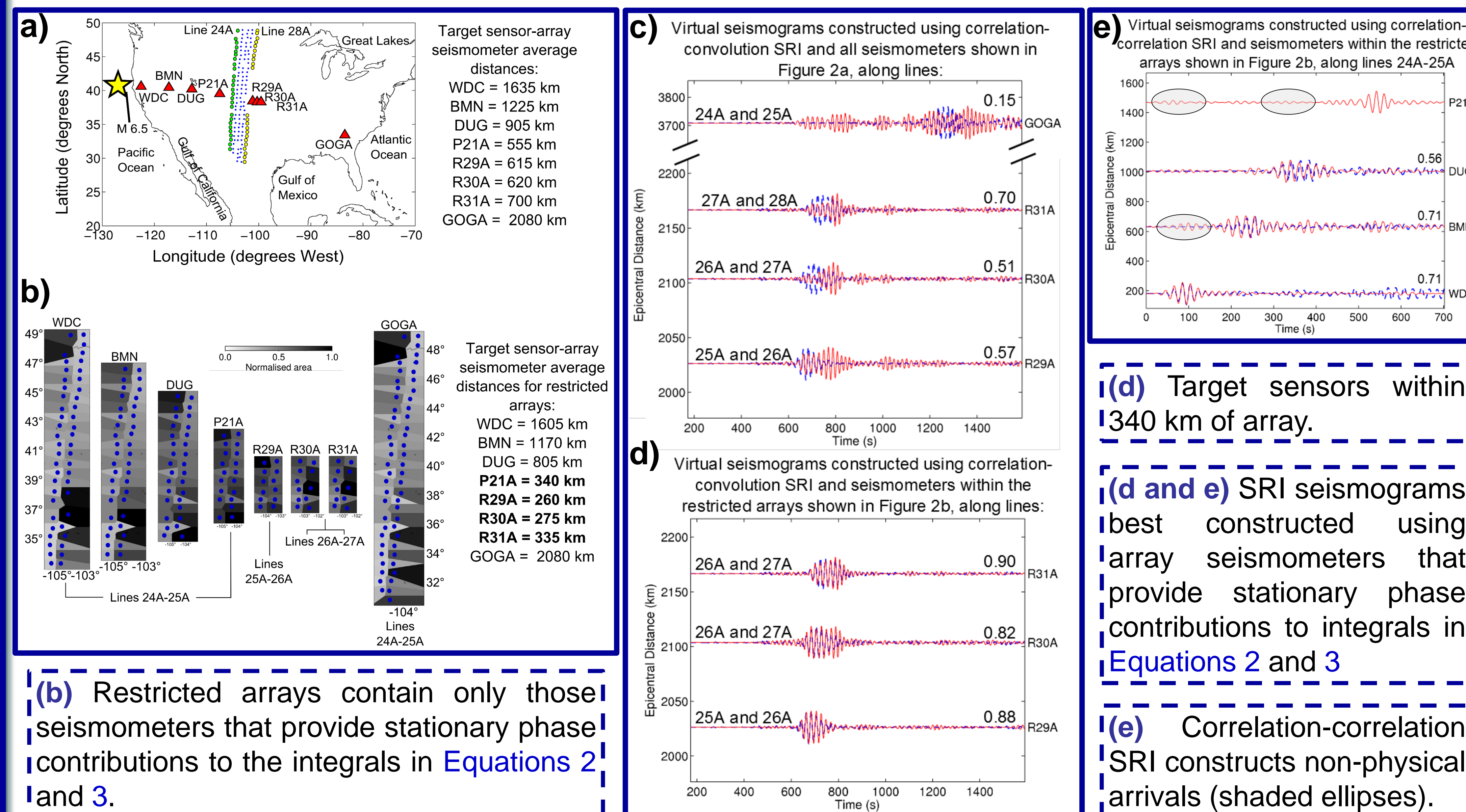


Figure 2: (a) Map of array seismometers (Lines 24A-28A, dots) and target sensors (triangles) on which virtual SRI seismograms of the M 6.5 earthquake (star) are constructed. (b) Spatially restricted seismometer arrays used for the SRI reconstructions in (d) and (e). Array seismometers are embedded within Voronoi cells (shaded polygons). (c) Virtual seismograms (red traces) constructed using correlation-convolution SRI (Equations 1 and 3) compared to real recordings of the event (blue traces) at target sensors R29A, R30A, R31A and GOGA. The full seismometer arrays shown in (a) are used to construct the SRI seismograms. Correlation coefficients, as listed above each trace, are low. (d) As (c) but SRI seismograms are constructed at R29A, R30A and R31A using the spatially restricted arrays shown in (b). Correlation coefficients are considerably higher when using the shorter arrays. (e) As (d) for virtual seismograms constructed using correlation-correlation SRI (Equations 1 and 2) at target sensors WDC, BMN, DUG and P21A.

## 4. Conclusions

Virtual earthquake seismograms are best constructed when:

1. Target sensors are located ~200 km – 500 km from array seismometers, and
2. The array seismometers provide stationary phase contributions to the SRI integrals.

- We construct virtual seismograms using both correlation-correlation and correlation-convolution SRI and find that the latter constructs fewer non-physical arrivals.
- Over the shortest target sensor-array seismometer distances only 12 array seismometers are required to construct reliable virtual seismograms (correlation coefficients up to 0.90).
- Over the largest length scales (e.g., to sensor GOGA), SRI is less successful due to attenuation in the medium and poorly constructed Green's functions  $G(x,r)$  by noise interferometry in Equation 1.